Eur Biophys J (1994) 23: 369–378

European Biophysics Journal

A fluorescence depolarization study of the orientational distribution of crossbridges in muscle fibres

Uulke A. van der Heide[1], Olaf E. Rem[1], Hans C. Gerritsen[1], Evert L. de Beer[2], Piet Schiereck[2], Ian P. Trayer[3], Yehudi K. Levine[1]

[1] Debye Institute, Department of Molecular Biophysics, University of Utrecht, Buys Ballot Laboratory, P.O. Box 80.000, 3508 TA Utrecht, The Netherlands
[2] Department of Medical Physiology, University of Utrecht, The Netherlands
[3] School of Biochemistry, University of Birmingham, UK

Received: 14 March 1994 / Accepted in revised form: 22 July 1994

Abstract. A fluorescence depolarization study of the orientational distribution of crossbridges in dye-labelled muscle fibres is presented. The characterization of this distribution is important since the rotation of crossbridges is a key element in the theory of muscle contraction. In this study we exploited the advantages of angle-resolved experiments to characterize the principal features of the orientational distribution of the crossbridges in the muscle fibre. The directions of the transition dipole moments in the frame of the dye and the orientation and motion of the dye relative to the crossbridge determined previously were explicitly incorporated into the analysis of the experimental data. This afforded the unequivocal determination of all the second and fourth rank order parameters. Moreover, this additional information provided discrimination between different models for the orientational behaviour of the crossbridges. Our results indicate that no change of orientation takes place upon a transition from rigor to relaxation. The experiments, however, do no rule out a conformational change of the myosin S1 during the transition.

Key words: Fluorescence – Muscle – Crossbridge

Introduction

The origin of the contractile force in muscle has been the subject of research throughout this century. The introduction of the sliding filament theory has proven to be a crucial breakthrough in the understanding of muscle contraction (Huxley 1957; Huxley 1957). In a contracting muscle actin and myosin filaments slide past each other without changing length. Twelve years later the rotating crossbridge model was proposed which suggests that the sliding of the filaments is brought about by a change of orientation of the crossbridges during a transition from weakly to strongly bound to the actin filament (Huxley 1969; Huxley and Simmons 1971).

Correspondence to: Y. K. Levine

Since the rotation of the crossbridges is a key element in the theory of muscle contraction, much research effort has been devoted to the characterization of the orientational distribution of the crossbridges in the strongly and weakly bound states. To this end fluorescence and phosphorescence depolarization techniques have been used extensively, however, without producing a consistent pattern (Cooke 1986; Thomas 1987, 1993).

A case in point are studies using probe molecules attached to the myosin SH1. In their earlier studies Ajtai and Burghardt reported distinct angular distributions of the long axes of the crossbridges relative to the fibre axis under rigor and in the presence of MgADP (Ajtai and Burghardt 1986). More recent work leads the same authors to conclude that the actin-bound crossbridges rotate predominantly about their long axes upon binding MgADP (Burghardt and Ajtai 1992; Ajtai et al. 1992). In contrast, other studies only find a broadening of the orientational distribution of the crossbridges and an increase in their mobility on a microsecond timescale upon binding ATP (Stein et al. 1990; Tanner et al. 1992). An added complication is that studies using fluorescent analogues of ATP suggest that no rotation of the crossbridges takes place (Yanagida 1985).

The comparison of all these studies is hampered by the fact that distinctly different models are used to describe the experimental data. For instance, the model introduced by Borejdo et al. (1982) explicitly assumes that the dye molecules attached to the crossbridges in the muscle fibre all have one and the same polar angle β relative to the fibre axis, but in the presence of a significant fraction of randomly oriented dye molecules. On the other hand in the double cone model used by Thomas and coworkers (Ludescher and Thomas 1988; Stein et al. 1990), the dye molecules are assumed to lie within a cone, which itself lies within a second cone at an orientation β relative to the fibre axis.

In this context it is important to note that the fluorescence depolarization does not yield direct information about the orientational distribution of the crossbridges in the muscle fibre. In principle the experiment only reveals

the second rank order parameters of the absorption and emission dipole moments and their 3 correlation functions. This limitation is a direct consequence of the fact that only dipole-allowed transitions are monitored because of the negligible contribution of multipole radiation to the fluorescence process (Birks 1970). A reliable interpretation of the experimental data in terms of the orientation of the crossbridges now requires the unambiguous determination of all the experimentally accessible information about the transition dipole moments.

A drawback of conventional fluorescence depolarization studies on muscle fibres is the use of a fixed 90° scattering geometry. These experiments yield 3 independent polarization ratios (Wilson and Mendelson 1983) and consequently cannot be used to disentangle the second rank order parameters and correlation functions. As the interpretation of the data is ambiguous, the extraction of the information about the orientational order in the fibre relies heavily on the formulation of models. In contrast, the order parameters and correlation functions can be extracted unequivocally from angle-resolved fluorescence depolarization data (Kooyman et al. 1981; Van der Meer et al. 1982; Van Gurp et al. 1988; Van der Heide et al. 1992 a). These angle-resolved fluorescence depolarization (AFD) experiments have been used for over a decade in studies of order and dynamics in macroscopically aligned lipid bilayers. This approach has also found applications for the determination of the directions of the transition moments in the molecular frame of fluorescent molecules embedded in stretched polymer films.

The order parameters and correlation functions of the transition dipole moments contain all the available information about the orientational order of the crossbridges in the muscle fibre. This information is, however, limited to the second and fourth rank order parameters of the crossbridges. In order to recover all of these order parameters we need to take into account the three factors contributing to the depolarization of the fluorescence (Van der Heide et al. 1992 a): *1)* the orientation of the crossbridges in the muscle fibre, *2)* the orientation and rotation of the dye molecule relative to the crossbridge and *3)* the directions of the transition dipoles in the frame of the dye. Knowledge of the latter two factors is a prerequisite in the recovery of the order parameters of the crossbridges and for this reason they have been characterized previously for the two cysteine binding dye molecules, 1,5-I-AEDANS and E5M (Van der Heide et al. 1992 a, b).

Here, we combine this knowledge with the order parameters and correlation functions determined from angle-resolved measurements for characterizing the order parameters of the crossbridges. To this end experiments were carried out on muscle fibres labelled with 1,5-I-AEDANS (5-iodoacetamido-ethyl-amino-naphthalene-a-sulphonic acid) and E5M (eosin-5-maleimide). Data sets were collected at different excitation wavelengths in order to utilize the various orientations of the absorption dipole moments in the dye molecules.

The fibres were studied in rigor and relaxation at a physiological ionic strength of 160 mM. In rigor, the majority of the crossbridges will be attached to the actin filament in the strong binding state, whereas in relaxation an equilibrium exists between weakly bound and unbound crossbridges. This equilibrium can be shifted by varying the ionic strength of the relaxation solution (Brenner et al. 1982). In order to maximize the differences between the two states we also studied fibres in relaxation at an ionic strength of 300 mM where the crossbridges are expected to be unbound. All data sets obtained from fibres in a given physiological state were analyzed simultaneously. This approach relies on the fact that the differences in the depolarization data arise solely from the different orientations of the transition dipoles in the frame of the dyes and the distinct orientations of 1,5-I-AEDANS and E5M relative to the S1 (Van der Heide et al. 1992 a).

The second and fourth rank order parameters of the crossbridges have been extracted from the depolarization ratios in a model independent way. However, the reconstruction of the orientational distribution function from these parameters calls for the use of models. We have here tested three models for consistency with the observed order parameters. The first model (A) postulates a population of crossbridges at a fixed orientation with an additional randomly oriented component. In the second model (B) the crossbridges are assumed to lie within a cone. The last model (C), based on the Maximum Entropy Method (Levine and Tribus 1979), yields the smoothest distribution function consistent with the order parameters.

Theory

a. Angle-resolved fluorescence depolarization

We shall now consider a steady-state AFD experiment on labelled muscle fibres aligned along the z-axis of the laboratory frame. The fibre is illuminated with polarized light while the polarization of the fluorescence emission is subsequently detected at various angles ψ relative to the direction of the incident light (Fig. 1). For dipole allowed transitions (Birks 1970), the excitation and emission probabilities of a given molecule are proportional to $(\hat{e}_i \cdot \hat{\mu})^2$ and $(\hat{e}_f \cdot \hat{\nu})^2$ respectively. Here $\hat{e}_i$ and $\hat{e}_f$ are the polarization of the incoming and detected light and $\hat{\mu}$ and $\hat{\nu}$ represent the absorption and emission dipole moments of the molecule.

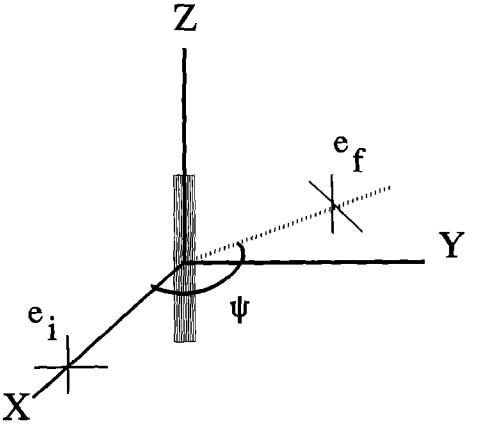

Fig. 1. The scattering geometry of the angle-resolved fluorescence depolarization experiment on a vertically mounted dye-labelled muscle fibre

The fluorescence intensity I_{if} can be expressed in terms of factors describing the molecular order and dynamics of the probe molecules in the sample and factors dependent on the geometry of the experiment (Van Gurp et al. 1988; Van der Heide et al. 1992 a). The explicit expressions for the intensities I_{hh}, I_{hv}, I_{vh} and I_{vv} for a vertically mounted fibre are

$$I_{hh}(\psi) \propto 1 - S_\mu - S_\nu + G_0 + 3\cos(2\psi)\, G_2\,, \tag{1a}$$

$$I_{hv}(\psi) \propto 1 - S_\mu + 2S_\nu - 2G_0\,, \tag{1b}$$

$$I_{vh}(\psi) \propto 1 + 2S_\mu - S_\nu - 2G_0\,, \tag{1c}$$

$$I_{vv}(\psi) \propto 1 + 2S_\mu + 2S_\nu + 4G_0\,. \tag{1d}$$

Here the first index denotes the direction of the excitation polarizer, vertical or horizontal, and the second index denotes the direction of the emission polarizer. The order parameters S_μ and S_ν are the second rank order parameters of the equilibrium orientational distribution of the absorption and emission dipole moments respectively. The correlation functions are determined by both the equilibrium orientational distribution and the rotational motion of the dye molecules between the time of absorption and emission. If the molecules do not rotate on the time scale of the fluorescence lifetime, the correlation function $G_k(t)$ are time independent and can be expressed in terms of linear combinations of the second and fourth rank order parameters (Van Gurp et al. 1988).

b. The extraction of the order parameters of the crossbridges

In this section we present the formal mathematical framework for the extraction of the order parameters of the crossbridges from the fluorescence depolarization experiments. To this end we shall separate three orientational transformations: *1)* the crossbridge relative to the fibre axis (Ω_x); *2)* the dye molecule relative to the crossbridge (Ω_R) and *3)* the transition dipole moments in the frame of the dye molecule (Ω_μ and Ω_ν), with Ω the Euler angles (α, β, γ). Furthermore we take into account the fact that the dye molecules 1,5-I-AEDANS and E5M move relative to the myosin S1 on a nanosecond timescale (Van der Heide et al. 1992 b). In contrast, the dynamics of the crossbridges in muscle fibres are too slow to be observed on the timescale of the fluorescence experiment (Stein et al. 1990).

Equations (1 a–d) show how the order parameters S_μ and S_ν for the absorption and emission dipole moments and the correlation functions G_0 and G_2 can be determined from the observed depolarization ratios. On using the closure relation of Wigner functions (Rose 1957; Zannoni 1979) we now find

$$S_\mu = \sum_{i,j=-2}^{2} \left\langle D^2_{0i}(\Omega_x)\right\rangle \left\langle D^2_{ij}(\Omega_R)\right\rangle D^2_{j0}(\Omega_\mu)\,, \tag{2a}$$

$$S_\nu = \sum_{l,m=-2}^{2} \left\langle D^{2*}_{0l}(\Omega_x)\right\rangle \left\langle D^{2*}_{lm}(\Omega_R)\right\rangle D^{2*}_{m0}(\Omega_\nu)\,, \tag{2b}$$

$$G_k = \sum_{ij,kl=-2}^{2} \left\langle D^{2*}_{kl}(\Omega'_x)\, D^{2*}_{lm}(\Omega'_R)\, D^2_{ki}(\Omega_x)\, D^2_{ij}(\Omega_R)\right\rangle \cdot D^{2*}_{m0}(\Omega_\nu)\, D^2_{j0}(\Omega_\mu)\,, \quad k = 0, 1, 2 \tag{2c}$$

with the order parameters of the crossbridges in the muscle fibre

$$\left\langle D^l_{mn}(\Omega_x)\right\rangle = \int \frac{\mathrm{d}\Omega_x}{8\pi^2}\, D^l_{mn}(\Omega_x)\, f_x(\Omega_x) \tag{3}$$

and the order parameters of the dye molecules in the crossbridge frame

$$\left\langle D^l_{mn}(\Omega_R)\right\rangle = \int \frac{\mathrm{d}\Omega_R}{8\pi^2}\, D^l_{mn}(\Omega_R)\, f_R(\Omega_R)\,. \tag{4}$$

Here $f_x(\Omega_x)$ is the orientational distribution of the crossbridges in the muscle fibre and $f_R(\Omega_R)$ is the orientational distribution of the dyes relative to the crossbridge.

The correlation functions (Eq. (2 c)) reflect the coupled stochastic motions of the dye molecules and the crossbridges in the muscle fibre. Here, Ω_x, Ω_R are the incoming and Ω'_x, Ω'_R the outgoing orientations. Now, the correlation functions G_k can be expressed as the product of the correlation functions of the crossbridge $G^X_{kl,ki}$ and of the dye molecules $G^D_{lm,ij}$

$$G_k = \sum_{ij,lm=-2}^{2} G^X_{ki,kj}\, G^D_{lm,ij}\, D^{2*}_{m0}(\Omega_\nu)\, D^2_{j0}(\Omega_\mu) \tag{5}$$

with

$$G^X_{ki,kj} = \left\langle D^{2*}_{kj}(\Omega'_x)\, D^2_{ki}(\Omega_x)\right\rangle \tag{6a}$$

and

$$G^D_{lm,ij} = \left\langle D^{2*}_{lm}(\Omega'_R)\, D^2_{ij}(\Omega_R)\right\rangle. \tag{6b}$$

The correlation functions of the crossbridge $G^X_{kl,ki}$ can be expressed as a linear combination of the second and fourth rank order parameters of the crossbridges in the muscle fibre (Zannoni et al. 1983; Van Gurp et al. 1988). The correlation functions of the dye molecules $G^D_{lm,ij}$ reflect the motions of the dye relative to the crossbridges. On assuming a mono-exponential fluorescence lifetime function $F(t) = \tau_F^{-1} \exp(-t/\tau_F)$, the time-averaged correlation function $G^D_{lm,ij}$ can be expressed as

$$G^D_{lm,ij} = \frac{\tau}{\tau + \tau_F}\left(G^D_{lm,ij}(0) - G^D_{lm,ij}(\infty)\right) + G^D_{lm,ij}(\infty)\,. \tag{7}$$

The correlation functions of the dye molecules at time $t = 0$ can be expressed as a linear combination of the second and fourth rank order parameters of the dye molecules relative to the crossbridges whereas at time $t = \infty$ they are equal to the product of the second rank order parameters (Zannoni et al. 1983; Szabo 1984; Van Gurp et al. 1988).

The angle-resolved geometry used in this study does not allow the determination of the correlation function G_1. However, this correlation function can be derived from the correlation function G_0 and G_2 and the steady-state fluorescence anisotropy (Zannoni et al. 1983) since

$$G_0(t) + 2G_1(t) + 2G_2(t) = P_2(\mu_{t=0} \cdot \nu_t)\,. \tag{8}$$

It is now clear that many parameters enter the analysis of the depolarization data. However, the orientations Ω_μ and Ω_ν as well as the orientational distribution function $f_R(\Omega_R)$ and the rotational correlation time τ are determined in separate experiments. Therefore, only the order parameters of

the crossbridges in the muscle fibre have to be extracted from the data.

It is important to stress that the explicit incorporation in the analysis of the orientation of the dye molecule relative to the crossbridge as well as the directions of the transition dipole moments of the dye molecules allows us to extract more order parameters than $\langle P_2 \rangle$ and $\langle P_4 \rangle$. In particular, the order parameters of rank 2 and 4 which depend on the rotation of the crossbridges about their long axes can now be recovered. This is indeed the merit of our approach to the analysis.

The non-zero order parameters entering the analysis are determined by the following symmetries:

1. The distribution function of the crossbridges is invariant under a rotation around the fibre axis (Z-axis). This implies that all α_x-dependent order parameters vanish so that $\langle D^l_{mn}(\Omega_x)\rangle = \langle D^l_{mn}(\Omega_x)\rangle \delta_{m0}$.
2. The distribution function of the crossbridges possesses mirror symmetry in the plane perpendicular to the fibre axis (XY) and the plane through the fibre axis (XZ). Consequently $\langle D^l_{mn}(\Omega_x)\rangle = (-1)^l \langle D^l_{mn}(\Omega_x)\rangle$, showing that all order parameters with odd l vanish. Furthermore $\langle D^l_{0n}(\Omega_x)\rangle = (-1)^n \langle D^l_{0-n}(\Omega_x)\rangle$.

Because no other symmetries can be assumed a priori, 8 distinct non-zero order parameters survive: $\langle D^l_{0n}\rangle$ with $l = 2, 4$ and $0 \le n \le l$. These parameters are optimized in the numerical analysis of the data. In order to satisfy the requirement of overdetermination, the data sets obtained from muscle in one physiological state and labelled following the same method were analyzed simultaneously using a global target approach (Arcioni et al. 1988).

c. *The interpretation of the order parameters*

The orientational distribution function f_x is characterized unambiguously only if the values of the order parameters of all ranks are known (Zannoni 1979; Johannson and Lindblom 1980). Since the fluorescence depolarization experiment does not contain information about order parameters of rank higher than 4, it is not possible to reconstruct an orientational distribution function in a model-independent way. Consequently, we have to postulate models for the orientational distribution function and test their consistency with the observed order parameters. Here we shall consider three models based on distinctly different premises.

In the first model (A) a fraction q of the dye molecules is taken to be randomly oriented in the muscle fibre with a fraction $1-q$ attached to the crossbridges. The crossbridges are taken to lie at a fixed orientation β_0, γ_0 thus forming a helical array in the fibre. This is similar to the model introduced by Borejdo et al. (1982). The order parameters can be obtained in a simple analytical form using (3).

In the second model (B) the crossbridges are assumed to lie within a cone whose axis is oriented at the Euler angles β_0, γ_0 relative to the fibre axis. Now we allow the crossbridges to deviate from this fixed orientation by $\pm\Delta\beta$, $\pm\Delta\gamma$. We note that since the dye molecules can move relative to the crossbridge, this model is similar to the double cone model proposed by Thomas and co-workers (Ludescher and Thomas 1988; Stein et al. 1990). The order parameters can now be obtained numerically from (3).

Finally, model C is the Maximum Entropy Form of the orientational distribution function (Levine and Tribus 1979). This is the smoothest possible form for the orientational distribution which is consistent with the experimentally accessible order parameters. This choice implies that the series expansion of the distribution function in terms of Wigner functions converges rapidly. In the absence of any other experimental information, we believe that this is the only approach for reconstructing a distribution free from any implicit assumptions. Again, the order parameters are evaluated numerically from (3).

Materials and methods

a. *Preparation of skinned muscle fibres*

Skinned muscle fibres from the psoas of rabbits were prepared according to the method described in De Beer et al. (1988). The rabbits were anaesthetized by means of pentobarbital sodium (30 mg/kg iv). Segments of the psoas muscle were dissected and rapidly frozen in liquid nitrogen in order to skin the fibres thermally. After 15 min, the frozen muscles were removed from the liquid nitrogen and stored on silica gel for at least 10 days at –25 °C (Stienen et al. 1983, 1985). Single fibres were easily obtained from the dried preparation.

b. *Solutions*

The muscle fibres were brought into the rigor, the relaxed or the activated state by soaking them in a solution with the appropriate concentrations of MgATP and Ca^{2+} (Table 1). Creatine kinase (CK) and creatine phosphate (CP) were added to the relaxation and activation solutions for the regeneration of ATP. In order to prevent degradation of CK, it was added to a concentration of 1 mg/ml just before use. The compositions of these solutions were calculated for a temperature of 25 °C according to the method described by Fabiato and Fabiato (1979). MOPS was used to buffer the solution at a pH of 6.8. The compositions of the solutions are listed in Table 1. MOPS and Na_2ATP were obtained from Sigma Chem. Co, CK and CP from Boeh-

Table 1. The composition of solutions. All solutions contain 10 mM MOPS and 20 mM EGTA. The pH was set at 6.8 using KOH. The ionic strength (I.S.) was adjusted by adding KCl

Solution	Na_2CP (mM)	Na_2ATP (mM)	$MgCl_2$ (mM)	$CaCl_2$ (mM)	I.S. (mM)
Rigor	–	–	1.38	–	160
Relaxation 160	12	5.84	6.62	–	160
Relaxation 300	12	5.84	6.62	–	300
Activation	12	6.05	6.24	20.12	160

ringer Mannheim GmbH (Mannheim, Germany) and all the other chemical from Merck (Darmstadt, Germany).

c. Labelling

Two different methods were used to label the myosin SH1 with 1,5-I-AEDANS or E5M (both obtained from Molecular Probes, Eugene, OR). The first method is a modification of that described by Borejdo and Putnam (1977). Essentially the method makes use of the observation (Duke et al. 1976) that the affinity of 1,5-I-AEDANS for the SH1 on S1 increases significantly under relaxing conditions, while that for the cys374 on actin decreases. It has been suggested that the reactivity of SH1 is much higher than that of other cysteines in the fibre so that a high specificity of the labelling is obtained. Borejdo et al. (1977) claim that more than 75% of the dye is attached to myosin SH1.

A skinned muscle fibre was mounted between two stainless steel clips and immersed in the relaxation 160 solution (Table 1) for 15 min.The fibre was then activated for 1 min and again relaxed for 15 min. At this stage the sarcomere length was measured by laser diffraction and set to 2.0 μm. The fibre was then labelled by immersing it for one hour in the relaxation 300 solution to which dye molecules were added to a concentration of 100 μM. Directly after labelling, the muscle fibre was washed three times in relaxation solution for 15 min in order to remove free dye molecules from the solution. Finally the fibre was kept in the relaxation solution for 12 h and was immediately used for experiments.

The second method (2) to label the SH1 is a modification of that described by Ludescher and Thomas (1988). In this method the cysteines in the fibre were first blocked with a non-fluorescent maleimide, N-ethyl-maleimide (NEM, Sigma Chem. Co., St. Louis, MO). This was carried out under rigor conditions so as to inhibit the reactivity of SH1. After washing out the free NEM, the fibre was immersed in the relaxation solution and labelled as in method 1. It has been suggested that at least 95% of the probes are bound to SH1 (Stein et al. 1990).

The striations of skeletal muscle can be easily imaged using an interference microscope. When the myosin S1 in a muscle is selectively labelled with fluorescent dye molecules, a fluorescence image will also reveal this striated pattern. Poor selectivity is manifested by a significant reduction of the contrast between the myosin and the actin bands. Confocal fluorescence microscope images of fibres labelled following methods 1 and 2 showed a clear striation throughout. This is an additional indication that the dye is predominantly located in the myosin band.

d. Tension development of labelled muscle fibres

A set-up similar to that described by De Beer et al. (1988) was used to monitor tension development in the labelled muscle fibres. The fibres were mounted between two stainless steel clips, one of which was attached to a strain gauge force transducer (AME 801, Aksjeselskapet Mikro Elektronikk). The maximum force developed was found to decrease at most by 20% after labelling the fibre with E5M or 1,5-I-AEDANS. Furthermore, the rate of force development was slowed down significantly. These findings are consistent with other studies (Borejdo and Putnam 1977), and indicate that the labelled muscle fibres retain their ability to develop tension.

e. The lay out of the angle-resolved fluorometer

The home-built angle-resolved fluorometer used in this study is based on that described in detail by Van Gurp et al. (1988) for studies of slab-shaped samples. However, studies of fibrillar systems impose additional demands on the sensitivity of the detection system and the stability of the alignment as a result of the small size of the sample. In order to obtain the required stability of the alignment, 9 identical emission lines are used, positioned at 9 angles ψ relative to the direction of the incident beam.

In the experiment it is essential that a narrow beam of polarized light illuminates the sample. Furthermore the fluorescence emission has to be detected with a high angular resolution. Here a trade-off has to be made between the numerical aperture of the optical system and the intensity of the detected fluorescence. In fluorescence studies of muscle fibres numerical apertures of up to 1.3 have been used frequently (Borejdo and Putnam 1977; Wilson and Mendelson 1983; Ajtai and Burghardt 1986). We have chosen to limit the numerical apertures at both the excitation and emission side to 0.04, corresponding to a cone with a half angle of 2.3°. This small value guarantees the angular resolution we consider essential in our experiment.

The lay out of the excitation line is similar to that described by Van Gurp et al. (1988), except that a slit is used to adjust the width of the spot to the size of the muscle fibre. A 1600 W Xenon arc lamp (OSRAM) is used as a light source. Narrow band ($\Delta\lambda \approx 10$ nm) interference filters (Schott, Mainz, Germany) are used to select an excitation wavelength suitable for a particular probe. The light is focused with a condenser lens (all lenses were obtained from Spindler & Hoyer, Göttingen, Germany) on a slit with a height of 8 mm and an adjustable width. A parallel beam is formed by passing the light through a lens with a diameter of 1 cm and a focal length of 30 cm. A Glan Taylor prism is used to polarize the light. The polarized light is subsequently focused on the muscle fibre with a lens of 1 cm diameter and a focal length of 15 cm. The muscle fibre is mounted in the centre of the experimental set-up. Each end of the fibre can be positioned independently with two *xyz*-translation tables (Newport, Irvine, CA). This is necessary to ensure a proper vertical alignment of the fibre in the focus of the excitation and emission lines. In order to limit the refraction of the polarized light at the interface with the muscle fibre the sample was placed in a cylindrical quartz cuvette with a diameter of 2.5 cm, filled with a buffer. Although it is not possible to obtain a perfect matching of the refractive indices of the buffer and the muscle fibre without affecting the functionality of the muscle fibre, we believe that the effects of refraction on the interface of the fibre are small. This can be justified a posteriori.

The fluorescence emission light first passes a sheet polarizer (Melles Griot, Irvine, CA) used as an analyzer. The fluorescence emission from the sample is then coupled into an optical fibre (Ensign Bickford, Avon, Conn.) with a single lens. The optical fibre is used as a light guide from the emission line to the detector. A small aperture in front of the detector ensures that only light from a given optical fibre is admitted to the detector. In this way the fluorescence is measured at the 9 angles sequentially using only a single detection system. Optical filters can be placed in front of the aperture for the selection of the fluorescence light and the rejection of scattering.

The detector consisted of a standard single-photon counting device in combination with a Philips P2020Q photo multiplier tube (Philips, Eindhoven, NL) operating at a voltage of 2500 V. The PMT was cooled to −10 °C with a Peltier element (Princeton Applied Research, Danvers, MA) in order to limit the thermal noise. The signal from the PMT was fed into a home made pre-amplifier and then passed to a discriminator (Elscint STD-N-2). The pulses from the discriminator are counted with a digital photometer (Spex Industries, Edison, NJ).

The data acquisition is controlled with a 286 PC. At any given angle ψ the fluorescence intensity is acquired in a series of time windows each 100 ms long. In this way both the average count rate as well as its standard deviation is determined experimentally. The total collection time is varied so as to obtain an accuracy of 1–3% independent of the absolute fluorescence intensity.

We shall henceforth consider the four distinct polarization ratio: $I_{hh}(\psi)/I_{hv}(\psi)$, $I_{hh}(\psi)/I_{vh}(\psi)$, $I_{vh}(\psi)/I_{vv}(\psi)$ and $I_{hv}(\psi)/I_{vv}(\psi)$. In these four ratios each intensity appears twice, so that each is given an equal weight in the analysis of the data. Only the polarization ratios $I_{hh}(\psi)/I_{hv}(\psi)$ and $I_{hh}(\psi)/I_{vh}(\psi)$ are linearly dependent on $\cos(2\psi)$, Eqs. (1a–d). The fluorescence emission is now detected as a function of the angle ψ (Fig. 1) relative to the excitation line. The angles are chosen in such a way that the intensity measurements are evenly distributed over the range of $\cos(2\psi)$ −1 to 1.

The fluorescence depolarization ratios were measured in all four quadrants of the *XY*-plane in order to check for artefacts arising from scattering and a non-vertical alignment of the fibre. These artefacts can be recognized because they distort the linear dependence of the polarization ratios on $\cos(2\psi)$. The effects of scattering can be removed by selecting an appropriate combination of excitation and emission filters, while the alignment of the fibre can be corrected by means of the two *xyz*-translation tables.

Results

The angle-resolved fluorescence depolarization from bundles of up to five dye-labelled fibres were used in the experiments in order to increase the fluorescence intensity. The non-linear least squares Marquart procedure (ZXSSQ) from the IMSL library was used for the optimization of the parameter values using a global target approach (Arcioni et al. 1988).

The fluorescence depolarization of each bundle of fibres was measured in three different physiological states: *1)* in rigor, where the crossbridges are strongly bound to the actin filament; *2)* in relaxation at a normal ionic strength of 160 mM and *3)* in relaxation at a high ionic strength of 300 mM. In the latter two states the crossbridges are in an equilibrium between the weakly bound and the unbound state. By increasing the ionic strength this equilibrium shifts towards the unbound state (Brenner et al. 1982). The data sets were collected at different excitation wavelengths in order to utilize the different orientations of the transition dipole moments in the dye molecule.

In all the data sets the fluorescence polarization ratios $I_{hh}(\psi)/I_{hv}(\psi)$ and $I_{hh}(\psi)/I_{vh}(\psi)$ exhibited a linear dependence on $\cos(2\psi)$ within the margin of error. Here ψ is the angle between the emission and the excitation axis. Furthermore, the ratios I_{vh}/I_{vv} and I_{hv}/I_{vv} were found to be independent of the angle ψ. This indicates that systematic errors, such as scattering and a non-vertical alignment of the bundle of muscle fibres did not compromise the experimental observations.

Distinctly different polarization ratios were obtained from experiments using 1,5-I-AEDANS and E5M labelled fibres in the same physiological state. A change in the wavelength of the excitation light also resulted in markedly different polarization ratios (Fig. 2). This underscores our expectation that the depolarization data reflect the orientational distribution of the transition dipole moments in the muscle fibre. It shows that the data not only depend

Table 2. Two methods for labelling muscle fibres with 1,5-I-AEDANS or E5M

Method 1	Method 2
	15 min rigor
	120 min rigor + 100 µM NEM + 20 mM $NaPP_i$
	2 times 15 min rigor
15 min relaxation 160	15 min relaxation 160
60 min relaxation 300 + 100 µM dye + 20 mM $NaPP_i$	60 min relaxation 300 + 100 µM dye + 20 mM $NaPP_i$
3 times 15 min relaxation 160	3 times 15 min relaxation 160
12 h relaxation 160	12 h relaxation 160

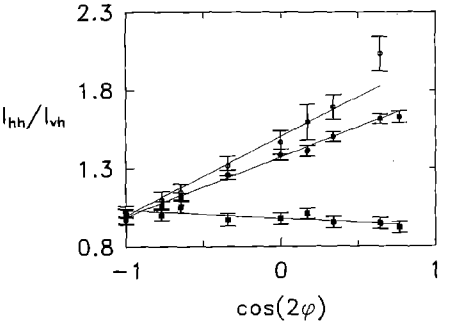

Fig. 2. Depolarization ratios of SH1 labelled muscle fibre. ○: 1,5-I-AEDANS, excitation wavelength 362 nm; ●: E5M, exc. 464 nm; ■: E5M, exc. 337 nm

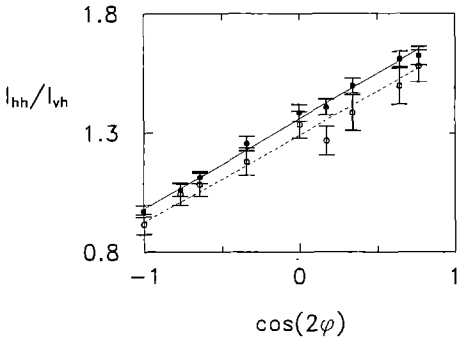

Fig. 3. The ratios I_{hh}/I_{vh} for a muscle fibre labelled at the SH1 with E5M, excitation wavelength 464 nm. ●: rigor; ○: relaxation 300

Table 3. The order parameters of the crossbridges in a muscle fibre labelled with 1,5-I-AEDANS and E5M

	Rigor	Relaxation 160	Relaxation 300
Method 1			
$\langle P_2 \rangle$	0.014±0.010	0.020±0.010	0.015±0.010
$\langle D^2_{02} \rangle$	0.010±0.010	0.023±0.010	0.017±0.010
$\langle P_4 \rangle$	−0.23±0.04	−0.20±0.05	−0.16±0.04
$\langle D^4_{02} \rangle$	−0.11±0.02	−0.11±0.02	−0.17±0.03
$\langle D^4_{04} \rangle$	0.13±0.08	0.11±0.09	0.02±0.06
Method 2			
$\langle P_2 \rangle$	0.000±0.010	0.000±0.010	−0.010±0.010
$\langle D^2_{02} \rangle$	0.000±0.010	0.021±0.015	0.040±0.015
$\langle P_4 \rangle$	−0.23±0.05	−0.19±0.05	−0.15±0.05
$\langle D^4_{02} \rangle$	−0.17±0.06	−0.13±0.02	−0.11±0.02
$\langle D^4_{04} \rangle$	0.08±0.08	0.10±0.06	0.04±0.06

on the orientational distribution of the crossbridges in the muscle fibre, but also on the orientations of these dipole moments in the dye frame and the orientational distribution of the dye relative to S1.

Remarkably, no significant differences were found in the data obtained from muscle fibres in rigor and relaxation 160, whereas the depolarization ratios from fibres in relaxation 300 only changed slightly (Fig. 3). Good fits of the 8 order parameters were obtained when the order parameters $\langle D^1_{0n} \rangle$ for odd values of n were taken to be 0. This is not a limitation, since these terms primarily describe the orientational distribution of the crossbridges around their long axes. Effectively, this means the data are consistent with an orientational distribution of the crossbridges in the muscle fibre possessing a 180° symmetry around the crossbridge axis.

The values for the 5 remaining order parameters are given in Table 3. For all the muscle fibres the values of the rank 2 order parameters $\langle P_2 \rangle$ and $\langle D^2_{02} \rangle$ were close to 0, whereas the order parameters $\langle P_4 \rangle$ and $\langle D^4_{02} \rangle$ were found to be negative for all the fibres. The order parameter $\langle D^4_{04} \rangle$ could only be determined within a large margin of error.

Reconstruction of the orientational distribution function

We shall now consider the reconstruction of the orientational distribution function from the order parameters listed in Table 3 for the directly labelled fibres (method 1) and fibres which were blocked with NEM prior to labelling (method 2). In particular, we test the three distinct models described above for their consistency with the order parameters.

As a first step we shall consider the information furnished by the order parameters $\langle P_2 \rangle$ and $\langle P_4 \rangle$ which are independent of the Euler angle γ. This corresponds to the information that is accessible when the orientations of the dye relative to the crossbridge and the transition dipole moments relative to the dye are not explicitly included in the analysis.

The parameters q and β_0 of model A shown in Table 4 provided a perfect fit to the order parameters $\langle P_2 \rangle$ and $\langle P_4 \rangle$, Table 3. As expected the fraction q of the randomly oriented population increases upon relaxation. On the other hand, the angle β_0 does not change significantly. This agrees well with the results reported by Wilson and Mendelson (1983). We note that the consistently lower values for q found here may be indicative of a more specific labelling.

In a similar way, model B is found to provide excellent fits to the two order parameters, Table 4. The position of the centre of the cone β_0 does not change upon relaxation of the muscle fibre. However, the width of the cone $\Delta\beta_0$ increases by about 5°.

The Maximum Entropy Form of the orientational distribution function consistent with the two order parameters $\langle P_2 \rangle$ and $\langle P_4 \rangle$ takes the form (Van Gurp et al. 1988).

$$f_x(\beta_x) = \exp(\lambda_2 P_2(\cos\beta_x) + \lambda_4 P_4(\cos\beta_x)) \quad (9)$$

The parameters λ_2 and λ_4 are listed in Table 4. Again, the position of the maximum of the distribution is found to be the same in rigor and relaxation, whereas the distribution is broader in relaxation.

Table 4. The model parameters of models A, B and C corresponding to the order parameters $\langle P_2 \rangle$ and $\langle P_4 \rangle$ in Table 3

	Rigor	Relaxation 160	Relaxation 300
Method 1			
Model A			
q	0.43	0.51	0.61
β_0	54	53	53
Model B			
β_0	53	52	52
$\Delta\beta$	22	25	27
Model C			
λ_2	−0.50	−0.22	−0.10
λ_4	−3.06	−2.38	−1.74
Method 2			
Model A			
q	0.41	0.51	0.60
β_0	55	55	56
Model B			
β_0	54	53	53
$\Delta\beta$	22	25	28
Model C			
λ_2	−0.73	−0.39	−0.30
λ_4	−3.19	−2.30	−1.69

The findings presented here show that widely differing models for the orientational distribution function of the crossbridges account for the same values of the order parameters $\langle P_2 \rangle$ and $\langle P_4 \rangle$. This clearly shows that knowledge of only these order parameters is not sufficient to discriminate between the models and also explains their profusion in the literature.

The additional rank two and four order parameters presented in Table 3 provide the key to resolving this unsatisfactory situation. We note once more that these parameters are obtained on explicitly including the orientations of the dye relative to the crossbridge and the transition dipole moments relative to the dye in the analysis. We have found that Models A and B fail to describe all 5 order parameters consistently and must therefore be discounted. In particular, it proved to be impossible to obtain a consistent fit of the values of both $\langle D^2_{02} \rangle$ and $\langle D^4_{02} \rangle$. The two order parameters depend on the angle of rotation of the crossbridges about their long axes as $\cos 2\gamma_x$ as well as on the polar angle β_x. The β_x dependent terms are fully determined by the values of $\langle P_2 \rangle$ and $\langle P_4 \rangle$. Consequently, the only degree of freedom for fitting these order parameters is the optimization of γ_0 for Model A and $\pm\Delta\gamma$ for Model B. We have been unable to find model parameters satisfying the constraints imposed by $\langle P_2 \rangle$ and $\langle P_4 \rangle$, which yield small values for $\langle D^2_{02} \rangle$ and simultaneously large negative values for $\langle D^4_{02} \rangle$. This situation can only be resolved on invoking a more sophisticated model such as the Maximum Entropy Form of the orientational distribution function. This distribution function, Model C, consistent with all the order parameters takes the form:

$$f_x(\beta_x, \gamma_x) = \exp(-U(\beta_x, \gamma_x)/kT) \tag{10a}$$

with

$$\begin{aligned} -U(\Omega_x)/kT = {} & \lambda_2 P_2(\cos\beta_x) + \lambda_4 P_4(\cos\beta_x) \\ & + \varepsilon(D^2_{02}(0, \beta_x, \gamma_x) + D^2_{0-2}(0, \beta_x, \gamma_x)) \\ & + \rho(D^4_{02}(0, \beta_x, \gamma_x) + D^4_{0-2}(0, \beta_x, \gamma_x)) \end{aligned} \tag{10b}$$

where λ_2, λ_4, ε and ρ are the parameters describing the strength of the potential. The results are listed in Table 5. Cross-sections of the distribution functions at $\gamma_x = 90°$ for the muscle fibres are shown in Fig. 4. The distribution functions for rigor, relaxation 160 and relaxation 300 all show a maximum at $\beta_x = 46 \pm 3°$. The full width half maximum is $22 \pm 3°$ for rigor and relaxation 300 and $27 \pm 3°$ for relaxation 300.

Table 5. The model parameters of model C corresponding to all order parameters in Table 3

	Rigor	Relaxation 160	Relaxation 300
Method 1			
λ_2	−0.58	−0.19	−0.16
λ_4	−3.59	−2.81	−2.24
ε	0.64	0.63	0.65
ρ	−1.24	−1.19	−1.71
Method 2			
λ_2	−1.14	−0.24	−0.43
λ_4	−4.54	−2.01	−2.82
ε	0.97	0.53	0.63
ρ	−2.04	−1.12	−1.38

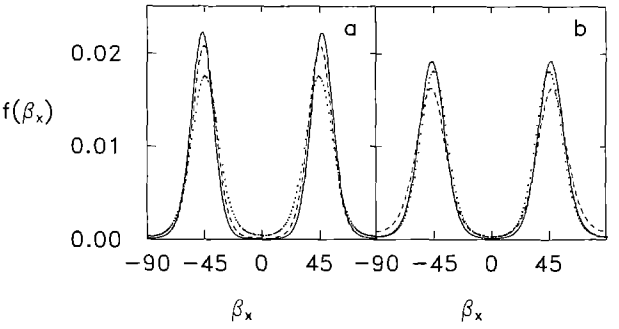

Fig. 4a, b. Cross-sections of the orientational distribution functions at $\gamma_x = 90°$. **a** Labelling method 1; **b** method 2; —: rigor; ---: relaxation 160; ···: relaxation 300

We note that the distribution function depends on the Euler angles β_x and γ_x, denoting the tilt angle of the crossbridge relative to the fibre axis and the orientation of the crossbridge around its internal axis respectively. However, the dependence on γ_x only enters the potential through the term $\cos(2\gamma_x)$ in the parameters $D^2_{0\pm2}(\Omega_x)$ and $D^4_{0\pm2}(\Omega_x)$. Consequently, only limited information can be obtained about the orientational distribution of the crossbridges around their long axis. Nevertheless, the γ_x dependent order parameters are indispensable for discriminating between the various models.

We have thus found that knowledge of 5 rank two and four order parameters affords a discrimination between different models for the orientational distribution function of the crossbridges. Nonetheless, it is not surprising that Model C provides a satisfactory description, since it has been constructed subject to the requirement of consistency with all the available order parameters. The question may now be posed as to whether Model C is unique. In addition it is known from the mathematical theory of the Maximum Entropy Formalism that it yields the broadest possible function. Nevertheless, any model which accounts for all 5 order parameters must reproduce a unimodal distribution. This leaves only the peak position and the width of the distribution as adjustable parameters. We have attempted to model the orientational distribution using Lorentzians, which can be used to describe sharply peaked functions. Surprisingly, this search yielded distribution functions indistinguishable from those of Model C. We believe that this is a strong indication that the distribution functions found with Model C can be considered to be reliable.

The results thus indicate that the crossbridges are highly ordered, and that no significant change of orientation of the crossbridges is observed between rigor and relaxation. The distribution corresponding to a fibre in relaxation 300 is slightly broader, reflecting the fact that a larger fraction of the crossbridges is unbound. Remarkably, the distribution functions obtained from fibres labelled directly (method 1) and fibres which were blocked with NEM prior to labelling (method 2) are similar and both sharply peaked. This suggests that the effects of non specific labelling are indeed negligible.

Discussion

The results presented here show that a reliable description of the orientational distribution of crossbridges in a muscle fibre can be extracted from fluorescence depolarization experiments, in a way independent of the dye molecules and transition dipole moments used in the experiment. The polarization ratios obtained at several excitation wavelengths and using two probes are distinctly different. Nevertheless, the data can all be described using the same orientational distribution. This indicates that the differences indeed arise from the orientation of the transition dipole moments in the frame of the dye molecules and the orientational distribution and rotational dynamics of the probe relative to the crossbridge.

The reliability of our approach is greatly enhanced by two factors. The angle-resolved fluorescence depolarization experiment allows the unequivocal determination of the order parameters of the transition dipole moments as well as two correlation functions. Furthermore, the global target analysis approach provides a convenient tool for checking the consistency of data sets obtained under different spectroscopic conditions. This stratagem ensures that a single solution of the numerical optimization can be found for describing all the available data. More importantly, the order parameters which depend on the rotation of the crossbridges about their long axes can now be recovered.

The goal of our study was the characterization of the orientational distributions of crossbridges in the rigor and relaxed states of muscle fibres. Our results indicate that no change of orientation takes place upon a transition between these two states. This finding does not support the conclusions from earlier studies in which a change of orientational distribution was reported (Ajtai and Burghardt 1986; Burghardt and Ajtai 1992; Ajtai et al. 1992; Stein et al. 1990; Tanner et al. 1992).

We believe that the differences between the conclusions arise primarily from the experimental characterization of more order parameters than simply $\langle P_2 \rangle$ and $\langle P_4 \rangle$. The extra order parameters allow us to discriminate between the various models. They have not been determined experimentally in previous studies and can only be obtained from angle-resolved experiments on making explicit use of the orientations of the transition dipole moments in the molecular frame and of the dye in the crossbridge frame. It is this additional data, derived from the experiments in a way free from any a priori assumptions, which allows us to discriminate between different models for the orientational behaviour of the crossbridges.

The similarity of the crossbridge orientations in rigor and relaxation is apparently at odds with the established ideas on the rotating crossbridge model that have dominated muscle research for many years (Huxley 1969; Huxley and Simmons 1971). These have postulated that a change of orientation of the whole of the S1 portion relative to the long pitch actin helix takes place upon a transition from the weakly to the strongly bound state. Nevertheless, our findings are supported by the electron microscopy study of Pollard et al. (1993), which suggests that the orientational distribution of the crossbridges in the intermediate states during the ATPase cycle is indistinguishable from the distribution found in rigor. Indeed these results appear to exclude any model in which states occurring early and late in the "powerstroke" have substantially different angles (e.g. 45° different) (Thomas 1993).

We note here that at a normal physiological strength of 160 mM only a small fraction of the crossbridges is in the weakly bound state with the rest unbound (Brenner et al. 1992). The surprising aspect is that the orientational distribution of the crossbridges in relaxation is so similar to that in rigor. A comparison between the weakly and strongly bound states thus calls for an in-depth study of the orientational distribution of the crossbridges at a range of ionic strengths from 20 to 300 mM along the lines set out in this study.

The recently published crystal structure of S1 and its model building, together with the crystal structure of actin may be the key for further understanding of the orientational behaviour of the crossbridges (Kabsch et al. 1990; Holmes et al. 1990; Rayment et al. 1993 a, b). This model suggests that local conformational changes in the main motor portion of the S1 head, as a result of ATP binding/hydrolysis and actin binding, cause the light chain-clad neck region of S1 to "wag" relative to this motor domain which remains attached to actin in both the weakly and strongly bound states in approximately the same orientation. Thus, the bulk of the head does not reorient during the energy transduction step, only the neck region (Rayment et al. 1993 b). Since the SH1 group is located in the main bulk of the motor domain close to the actin-S1 interface, any dye molecule located at this site would not be expected to sense the conformational rearrangements experienced by other parts of S1. Our results, therefore, are consistent with this model and point a way forward of how to test these ideas using dye molecules which are attached to sites on the myosin S1 that are proposed to experience the reorientation e.g. the myosin light chains.

References

Ajtai K, Burghardt TP (1986) Observation of two orientations from rigor cross-bridges in glycerinated muscle fibers. Biochemistry 25: 6203–6207

Ajtai K, Ringler A, Burghardt TP (1992) Probing cross-bridge angular transitions using multiple extrinsic reporter groups. Biochemistry 31: 207–217

Arcioni A, Tarrroni R, Zannoni C (1988) Fluorescence depolarization in liquid crystals. In: Polarized spectroscopy of ordered systems. Samori' B, Thulstrup EW (eds) Kluwer, Dordrecht, pp 421–453

Birks JB (1970) Photophysics of aromatic molecules. Wiley-Interscience, London

Borejdo J, Putnam S (1977) Polarization of fluorescence from single skinned glycerinated rabbit psoas fibers in rigor and relaxation. BBA 459: 578–595

Borejdo J, Assulin O, Ando T, Putnam S (1982) Cross-bridge orientation in skeletal muscle measured by linear dichroism of an extrinsic chromophore. J Mol Biol 158: 391–397

Brenner B, Schoenberg M, Chalovitch JM, Greene LE, Eisenberg E (1982) Evidence for cross-bridge attachment in relaxed muscle at low ionic strength. Proc Natl Acad Sci, USA 79: 7288–7294

Burghardt TP, Ajtai K (1992) Mapping global angular transitions of proteins in assemblies using multiple extrinsic reporter groups. Biochemistry 31: 200–206

Cooke R (1986) The mechanism of muscle contraction. CRC Rev Biochem 21: 53–118

De Beer EL, Gründeman RLF, Wilhelm AJ, Caljouw CJ, Klepper D, Schiereck P (1988) Caffeine suppresses length dependency of Ca^{2+} sensitivity of skinned striated muscle. Am J Physiol 254: C491–C497

Duke J, Takashi R, Ue K, Morales M (1976) Reciprocal reactivities of specific thiols when actin binds to myosin. Proc Natl Acad Sci, USA 73: 302–306

Fabiato A, Fabiato F (1979) Calculator programs for computing the composition of the solution containing multiple metals and ligands used for experiments in skinned muscle cells. J Physiol (Paris) 75: 463–505

Holmes KC, Popp D, Gebhard W, Kabsch W (1990) Atomic model of the actin filament. Nature 347: 44–49

Huxley AF (1957) Muscle structure and theories of contraction. Progr Biophys 7: 255–318

Huxley HE (1957) The double array of filaments in cross-striated muscle. J Biophys Biochem Cytol 3: 631–647

Huxley HE (1969) The mechanism of muscular contraction. Science (Wash. D.C.) 164: 1356–1366

Huxley AF, Simmons RM (1971) Proposed mechanism of force generation in striated muscle. Nature 233: 533–538

Johansson LBÅ, Lindblom G (1980) Orientation and mobility of molecules in membranes studied by polarized light spectroscopy. Q Rev Biophys 13: 63–118

Kabsch W, Mannherz HG, Suck D, Pai EF, Holmes KC (1990) Atomic structure of actin: DNase I complex. Nature 347: 37–44

Kooyman RPH, Levine YK, Van der Meer BW (1981) Measurement of second and fourth rank order parameters by fluorescence polarization experiments in a lipid membrane system. Chem Phys 60: 317–326

Levine RD, Tribus M (1979) The Maximum Entropy Formalism. MIT Press, Cambridge

Ludescher RD, Thomas DD (1988) Microsecond rotational dynamics of phosphorescent-labeled muscle crossbridges. Biochemistry 27: 3343–3351

Pollard TD, Bhandari D, Maupin P, Wachsstock D, Weeds AG, Zot HG (1993) Direct visualization by electron microscopy of the weakly bound intermediates in the actomyosin adenosine triphosphatase cycle. Biophys J 64: 454–471

Rayment I, Rypniewski WR, Schmidt-Basl K, Smith R, Tomchick DR, Benning MM, Winkelmann DA, Wesenberg G, Holden H (1993a) Three-dimensional structure of myosin subragment-1: a molecular motor. Science 261: 50–58

Rayment I, Holden H, Whittaker M, Yohn CB, Lorenz M, Holmes KC, Milligan RA (1993b) Structure of the actin-myosin complex and its implications for muscle contraction. Science 261: 58–65

Rose ME (1957) Elementary Theory of Angular Momentum. Wiley, New York

Stein RA, Ludescher RD, Dahlberg PS, Fajer PG, Bennett RLH, Thomas DD (1990) Time-resolved rotational dynamics of phosphorescent-labeled myosin heads in contracting muscle fibers. Biochemistry 29: 10023–10031

Stienen GJM, Gueth K, Rüegg JC (1983) Force and force transients in skeletal muscle fibres of the frog skinned by freeze-drying. Pfluegers Arch 397: 272–276

Stienen GJM, Blangé T, Treijtel BW (1985) Tension development and calcium sensitivity in skinned muscle fibres of the frog. Pfluegers Arch 405: 19–23

Szabo A (1984) Theory of fluorescence depolarization in macromolecules and membranes. J Chem Phys 81: 150–162

Tanner JW, Thomas DD, Goldman YE (1992) Transients in orientation of a fluorescent crossbridge probe following photolysis of caged nucleotides in skeletal muscle fibres. J Mol Biol 223: 185–203

Thomas DD (1987) Spectroscopic probes of muscle rotation. Annu Rev Physiol 49: 891–909

Thomas DD (1993) Pollard to actomyosin: "Freeze! Don't even move your head". Biophys J 64: 297–298

Van der Heide UA, Orbons B, Gerritsen HC, Levine YK (1992a) The orientation of transition moments of dye molecules used in fluorescence studies of muscle systems. Eur Biophys J 21: 263–272

Van der Heide UA, Gerritsen HC, Trayer IP, Levine YK (1992b) Determination of the orientation of fluorescent labels relative to myosin S1 in solution from time resolved fluorescence anisotropy experiments. SPIE Meeting on Time resolved Laser Spectroscopy in Biochemistry III. SPIE 1640: 681–689

Van der Meer W, Kooyman RHP, Levine YK (1982) A theory of fluorescence depolarization in macroscopically ordered membrane systems. Chem Phys 66: 39–50

Van Gurp M, Van Langen H, Van Ginkel G, Levine YK (1988) Angle-resolved techniques in studies of organic molecules in ordered systems using polarized light. In: Polarized spectroscopy of ordered systems. Samori' B, Thulstrup EW (eds) Kluwer, Dordrecht, pp 455–489

Wilson MGA, Mendelson RA (1983) A comparison of order and orientation of crossbridges in rigor and relaxed muscle fibers using fluorescence polarization. J Musc Res Cell Mot 4: 671–693

Yanagida T (1985) Angle of active site of myosin heads in contracting muscle during sudden length changes. J Musc Res Cell Mot 6: 43–52

Zannoni C (1979) Distribution functions and order parameters. The Molecular Physics of Liquid Crystals. Luckhurst GR, Gray GW (eds) Academic Press, London, pp 51–84

Zannoni C, Arcioni C, Cavatorta P (1983) Fluorescence depolarization in liquid crystals and membrane bilayers. Chem Phys Lip 32: 179–250